Hindawi Publishing Corporation
International Journal of Photoenergy
Volume 2008, Article ID 267345, 7 pages
doi:10.1155/2008/267345

Research Article

Thermal Behavior of $TiO_{2-x}N_x$ Nanostructured Powder

Vladimír Balek,[1] Jan Šubrt,[2] Hiroshi Irie,[3] and Kazuhito Hashimoto[3,4]

[1] *Nuclear Research Institute Řež, plc., 25068 Řež, Czech Republic*
[2] *Institute of Inorganic Chemistry, Academy of Sciences of the Czech Republic (AS CR), 25068 Řež, Czech Republic*
[3] *Graduate School of Engineering, The University of Tokyo, 7-3-1 Hongo, Bunkyo-ku, Tokyo 113-8656, Japan*
[4] *Research Center for Advanced Science and Technology, The University of Tokyo, 4-6-1 Komaba, Meguro-ku, Tokyo 153-8904, Japan*

Correspondence should be addressed to Jan Šubrt, subrt@iic.cas.cz

Received 3 September 2007; Accepted 7 December 2007

Recommended by M. Sabry A. Abdel-Mottaleb

Diffusion structural analysis (DSA), based on the measurement of the release of radon previously incorporated into the samples, was used to characterize thermal behavior of N-doped titania powder prepared by heat treatment of anatase in gaseous ammonia at 575°C and the reference TiO_2 powder prepared from the ST-01 anatase titania powder (Ishihara Ltd., Japan). The results of DSA, surface area and porosity measurements by nitrogen adsorption, SEM micrographs, XPS, and XRD are presented and discussed. The results of DSA are in agreement with the results of other methods and indicated the annealing of the subsurface structure irregularities of the samples. Transport properties of the samples were determined from the mobility of radon atoms released on sample heating in air. The decrease of radon permeability in the porous titania powders in the temperature range 850–1000°C due to annealing of the subsurface structure irregularities, that served as radon diffusion paths in the samples, was evaluated from the DSA results.

Copyright © 2008 Vladimír Balek et al. This is an open access article distributed under the Creative Commons Attribution License, which permits unrestricted use, distribution, and reproduction in any medium, provided the original work is properly cited.

1. INTRODUCTION

Titanium dioxide attracted a great attention since Fujishima and Honda [1] discovered in 1972 the photocatalytic splitting of water on TiO_2 electrode. Recently, the application of TiO_2 focused on environmental remediation, especially water detoxification and air purification [2–4]. TiO_2 is an efficient photocatalyst, but UV light is necessary for its activation. Solar energy contains only about 4% UV light and much of the rest is visible light.

In order to utilize the visible (solar) light efficiently for the photocatalytic reactions, titanium dioxide has to be modified. There have been several approaches how to modify TiO_2. Several authors [5–9] substituted Ti^{4+} in TiO_2 by Cr^{3+} or V^{3+} (V^{4+}) by metal ion implantation. It was demonstrated that the absorption band of Cr^{3+}-doped TiO_2 shifted and that NO_x decomposed giving rise to N_2, O_2, and N_2O as the result of the photocatalytic reaction under visible light irradiation with wavelength larger than 450 nm. It was reported [10–13] that it is possible to prepare the "oxygen-vacancy-based visible-light-sensitive titania" by the treatment of anatase under reductive hydrogen plasma.

N-doped titania photocatalyst sensitive to visible light irradiation was described in 2001 by Asahi et al. [14]. Since then, various types of TiO_2 doped with anions but for nitrogen such as sulfur and carbon have been widely studied [15–23].

The purpose of this study is to characterize the thermal behavior of N-doped porous titania powder under in situ conditions of heating to 1050°C in air and to reveal differences in the annealing of porosity and subsurface structure defects. The diffusion structural analysis (DSA) [24, 25] was used to this aim. The DSA is based on the measurement of radon release rate from samples previously labelled, where radon atoms serve as a microstructure probe. In our previous studies, the DSA was already used to monitor the microstructure development of titania powders as well as titania gel layers [25] during heating of their precursors in various gas media.

2. EXPERIMENTAL

2.1. Preparation of samples

Two samples were investigated in this study: a reference sample of nondoped titania powder (called sample A) prepared by heating of anatase powder, type ST-01, Ishihara Sangyo Kaisha, Ltd., Japan, (surface area 311 m^2/g) at 550°C in air

for 3 hours, and N-doped titania (called sample B) prepared by heating of the anatase powder (sample A) under NH_3 gas flow at 575°C for 3hours.

The chemical composition of the N-doped titania estimated by Irie et al. [23] was $TiO_{2-x}N_x$, where $x = 0.011$. The value of x was determined as the ratio of the XPS peak areas corresponding to 396 eV and 531 eV.

2.2. Methods

Scanning electron microscope (SEM) equipment by Philips, type XL 30CP, was used to characterize surface morphology.

Diffusion structural analysis (DSA) measurements were carried out by using the modified equipment NETZSCH DTA model 409 (NETZSCH, Selb, Germany) [26]. The radon-labelled titania powder (sample amount of 0.05 g) was situated in a corundum crucible and heated in air in the temperature range 20–1050°C at the rate of 6°C/min. The constant air flow (flow rate 50 mL/min) took the radon released from the sample into the measuring chamber of radon radioactivity.

The DSA results are presented as temperature dependencies of radon release rate E (in relative units); $E = A_\alpha / A_{total}$, where A_α is α-radioactivity of radon released in unit time from the labelled sample and A_{total} is total γ-radioactivity of the labelled sample. The A_{total} value is proportional to the rate of radon formation in the sample. Semiconductor and NaI (Tl) detectors were used for the α- and γ-radioactivity measurements, respectively.

2.3. Labelling of samples for DSA measurements

Samples for DSA measurements were labelled by ^{220}Rn using recoil energy 85 keV/atom during spontaneous α-decay of radionuclides ^{228}Th and ^{224}Ra adsorbed as nitrates in trace amount on the sample surface from acetone solution. The specific activity of the sample was 10^5 Bq/gram. The depth of ^{220}Rn ions implantation by the recoil energy of 85 keV into the anatase was 60 nm from the surface of sample grains as calculated by means of Monte Carlo method using TRIM code [27]. It has been supposed that ^{220}Rn atoms formed by the spontaneous α-decay of ^{228}Th and ^{224}Ra were trapped in the subsurface layers of the sample and that structural irregularities served as diffusion paths for the radon atoms released by diffusion. The mechanisms of radon diffusion in open pores, intergranular space, or interface boundaries, respectively, were supposed to control the release of the radon from the sample.

In general, the increase in the radon release rate, E, may characterize an increase of the surface area of interfaces or porosity, whereas a decrease in E may reflect processes like closing up structure irregularities that serve as paths for radon migration, closing pores, and/or a decrease in the surface area of the interfaces.

The advantage of the DSA application consists in the possibility to characterize the microstructure changes under in situ conditions of sample heating in a selected gas environment and to bring about information about transport properties of the samples.

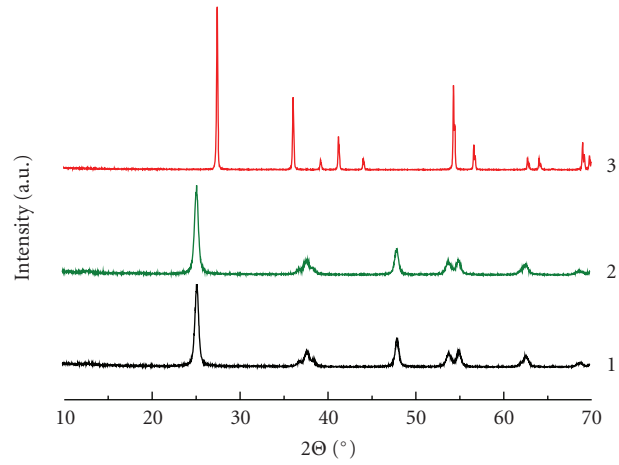

Figure 1: XRD patterns of the starting TiO_2 (sample A) and $TiO_{2-x}N_x$ (sample B) heated to various temperatures: (1) starting TiO_2 prepared from anatase ST 01, Ishihara Ltd., Japan (sample A), (2) $TiO_{2-x}N_x$ (sample B) prepared by heating sample A in a flow of NH_3 at 575°C/3 h, and (3) $TiO_{2-x}N_x$ (sample B) annealed at 950°C.

3. RESULTS AND DISCUSSION

3.1. Microstructure characterization

From the XRD pattern in Figure 1 (curve 2), it followed that the N-doped sample investigated in this study was homogeneous anatase, as no peaks of TiN were observed. It was found that values of BET surface area and porosity of sample B increased in comparison with sample A. The etching of nondoped titania powder at the temperature of 575°C with ammonia gas caused an increase of its surface area from 63 to 151 m^2/g, and thetotal porosity volume increased from 0.36 to 0.84 cm^3/g (see Table 1).

SEM micrographs in Figure 2 characterized the surface morphology of samples A and B, respectively.

DSA results in Figure 3 were used to characterize the thermal behavior of the samples, their permeability for radon atoms, and microstructure changes on heating in air.

We assumed that the increase of the radon release rate, E, observed in Figure 3 in the temperature range 50–800°C was due to the radon diffusion along structure irregularities in subsurface of the grains. The random "single-jump" diffusion mechanism of radon was supposed to control the release of radon in this temperature range.

From Figure 3, it followed that the slope of the respective DSA curves slightly differed in this temperature range. The increased slope of the radon release rate, E, was observed with N-doped titania sample during air heating. It is in a good agreement with the higher values of total porosity and surface area found for sample B in comparison with reference sample A (see Table 1). From the observed decrease of the radon release rate, $E(T)$, it followed that annealing of microstructure irregularities took place with both samples A and B on heating in the temperature range 850–1000°C accompanied by a decrease of surface area and porosity.

Table 1: Surface area and porosity of TiO_2 and $TiO_{2-x}N_x$ nanostructured powders.

Sample	Phases composition by XRD	Surface area by BET m^2/g	Total porosity volume cm^3/g
Starting TiO_2-sample A	Anatase	63.3	0.357
$TiO_{2-x}N_x$-sample B	Anatase	151	0.839
$TiO_{2-x}N_x$-sample B annealed to 950°C	Rutile	2.7	0.016

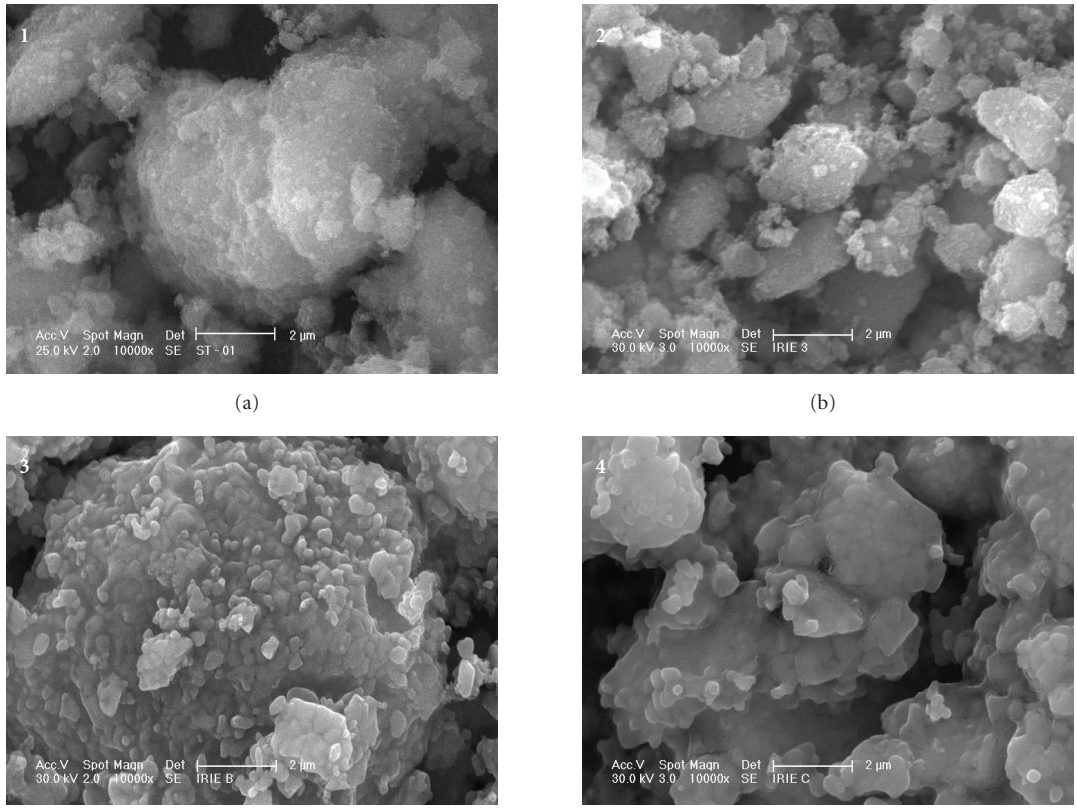

Figure 2: SEM micrographs of starting TiO_2 (sample A) and $TiO_{2-x}N_x$ (sample B) heated to various temperatures: (1) starting TiO_2 prepared from anatase ST 01, Ishihara Ltd., Japan, (2) $TiO_{2-x}N_x$ (sample B) prepared by heating sample A in a flow of NH_3 at 575°C/3 h, (3) $TiO_{2-x}N_x$ (sample B) annealed at 800°C, and (4) $TiO_{2-x}N_x$ (sample B) annealed at 950°C.

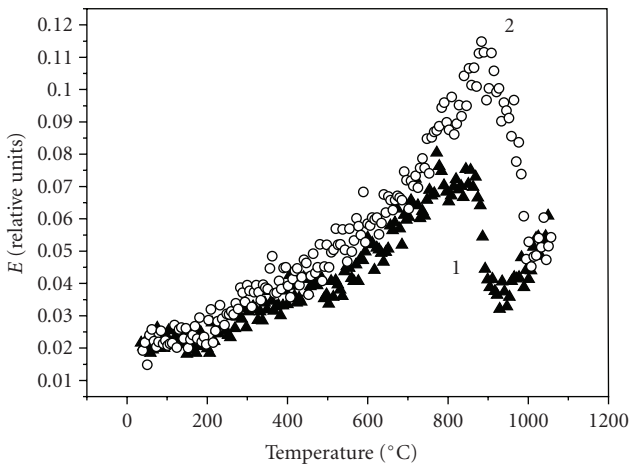

Figure 3: DSA results of sample A (curve 1) and sample B (curve 2) measured during heating in air at the rate of 6 K/min.

The surface area and porosity values of sample B annealed to 950°C decreased to 2.7 m^2/g and 0.016 cm^3/g, respectively.

Growth of crystallites of the samples on heating from 800 to 950°C was confirmed by the SEM micrographs (see Figure 2). Moreover, from the XRD pattern in Figure 1 (curve 3), it followed that in sample B annealed to 950°C the crystal transformation into rutile took place. In this respect, the DSA results (see Figure 3) monitored the anatase-rutile transition and the grain growth of the rutile particles during sample heating. The XRD and SEM micrographs confirmed the interpretation of the DSA results. From the XRD patterns presented in [28–30], it followed that the anatase-rutile transition took place on heating to the temperatures 800–900°C.

Figure 4 depicts XPS spectra of the N-doped titania heated to 800°C and 950°C, respectively. By means of X-ray photoelectron spectroscopy, it was demonstrated that the presence of the nitrogen atoms was no more indicted in the sample heated to 950°C.

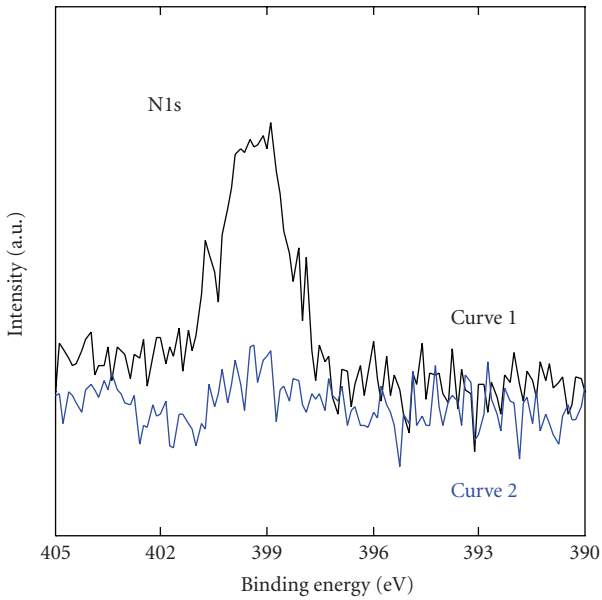

Figure 4: XPS spectra of the N-doped titania (sample B) heated to 800°C (curve 1) and 950°C (curve 2).

The microstructure development of the samples on heating was quantitatively described by the mathematical model [31, 32] supposing that pores and subsurface structure defects served as paths for radon diffusion. The application of the model enabled us to evaluate transport properties of the N-doped titania in comparison with the properties of the reference nondoped titania powder.

3.2. Transport properties of porous titania

It has been supposed that ^{220}Rn atoms were incorporated to the depth of 60 nm from the surface and trapped in the subsurface of the sample; the structural irregularities served as paths for the radon atoms released by diffusion. We assumed that the increase of the radon release rate, E, observed in the temperature range 50–800°C (see Figure 3) was due to the radon diffusion along structure irregularities in subsurface layers of the grains. The random "single-jump" diffusion mechanism of radon was supposed to control the release of radon in this temperature range.

The radon release rate, $E(T)$, can be written as [31]

$$E(T) = E_R + E_D(T)\cdot\Psi(T). \tag{1}$$

The term E_R is radon release rate due to recoil and the term E_D is radon release rate due to the diffusion, depending on the number of radon diffusion paths. The term E_D characterizes radon permeability along structure irregularities serving as diffusion paths, and $\Psi(T)$ is the function characterizing the decrease of the number of the radon diffusion paths. The advantage of the DSA application consists in the possibility to characterize microstructure changes under insitu conditions of sample heating in a selected gas environment and to bring about information about transport properties of the samples.

In the evaluation of the DSA results, it was supposed that radon atoms can migrate along several independent paths, such as micropores, intergranular space, as well as interface boundaries. Consequently, the mechanism of radon diffusion along two independent paths of the porous titania was considered. The following expression was used to describe the temperature dependence of the radon release rate E_D, due to diffusion:

$$E_D = \left(\frac{3}{y}\right)\left(\coth y - \left\{\frac{1}{y}\right\}\right),$$
$$y(T) = \left(\frac{(S/M)\rho}{(D/\lambda)^{1/2}}\right), \tag{2}$$

where S/M is surface area of open pores, intergranular space, and interfaces serving as radon diffusion paths, ρ is density of the sample, $(D/\lambda)^{1/2}$ is average radon diffusion length, D is radon diffusion coefficient, and λ is radon decay constant ($\lambda = 0.00127\ s^{-1}$);$D = D_0 \exp(-Q_D/RT)$, where D_0 is the factor depending on the number of diffusion paths and their availability for radon atoms migration, Q_D is activation energy of radon migration involving both the activation energy of the escape of radon atoms from the traps in the solid sample and that of the migration along diffusion paths in the solid.

In the mathematical model used in this study for the evaluation of DSA results, it was supposed that the decrease in the temperature dependence of the radon release rate, $E_D(T)$, reflected a decrease of the number of radon diffusion paths.

The following expression for $\Psi(T)$ functions was proposed [27] to describe the decrease of the number of radon diffusion paths due to changes of the microstructure:

$$\Psi(T) = 0.5\left[1 + \operatorname{erf}\frac{1 - T_m/T}{\Delta T\sqrt{2}/T}\right], \tag{3}$$

where erf is the sign for the integral Gaussian function, T_m is the temperature of maximal rate of the annealing of the defects that serve as radon diffusion paths, and ΔT is the temperature interval of the respective solid state process.

3.3. Comparison of experimental DSA results with the model curves

It was demonstrated by DSA results (see Figures 5(a) and 5(b)) that the etching nondoped titania powder at the temperature of 575°C with ammonia gas caused changes in radon permeability in subsurface of samples. Radon diffusion parameters were calculated from the DSA results (see Table 2).

From Figures 5(a) and 5(b), it followed that experimental DSA results and model curves of the temperature dependences of the radon release rate are in a good agreement. The DSA results characterized differences in the annealing of subsurface structure irregularities, serving as radon diffusion paths in titania powders.

The experimental DSA results were evaluated by means of the mathematical model, supposing that nanopores and subsurface structure irregularities served as paths for radon

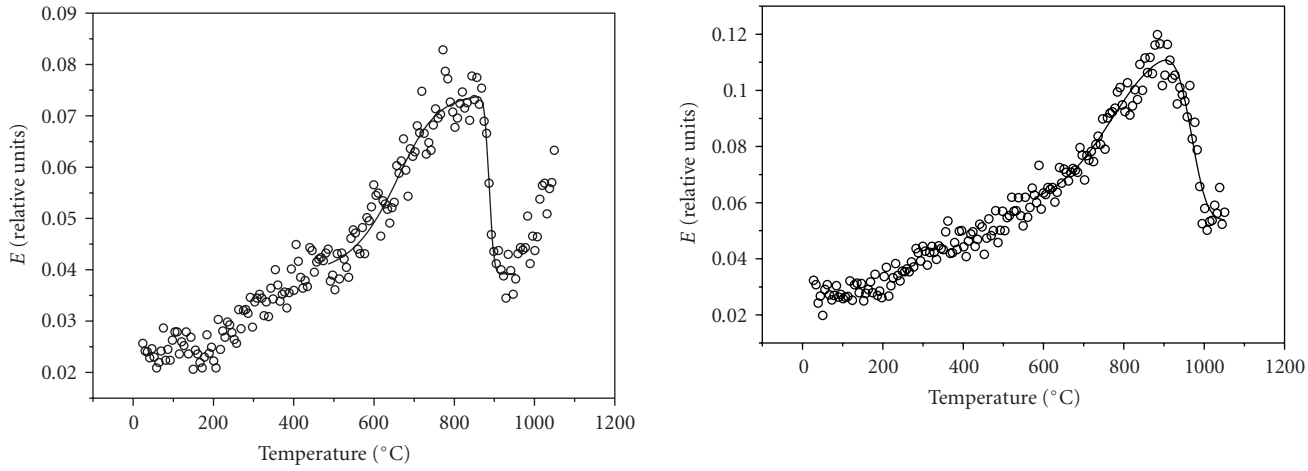

Figure 5: DSA experimental results (round points) and the results obtained by mathematical modeling and fitting with the experimental results (full lines) for the samples; (a) nondoped TiO_2 prepared from anatase ST 01, Ishihara Ltd., Japan, (b) sample B prepared by heating sample A in a flow of NH_3 at 575°C/3 h.

Table 2: Characteristics of radon permeability of TiO_2 and $TiO_{2-x}N_x$ evaluated from DSA results.

Sample notation and preparation	Radon permeability characteristics Temperature range 20–450°C	
	D_0 (cm^2/s)	Q_D (kJ/mol)
Sample A: TiO_2 prepared from anatase ST 01 Ishihara Ltd. by heating at 550°C for 3 h in air	$8.4 \cdot 10^{-10}$	64 ± 5
Sample B: $TiO_{2-x}N_x$ prepared by heating sample A in a flow of NH_3 at 575°C for 3 h	$1.8 \cdot 10^{-11}$	42 ± 5

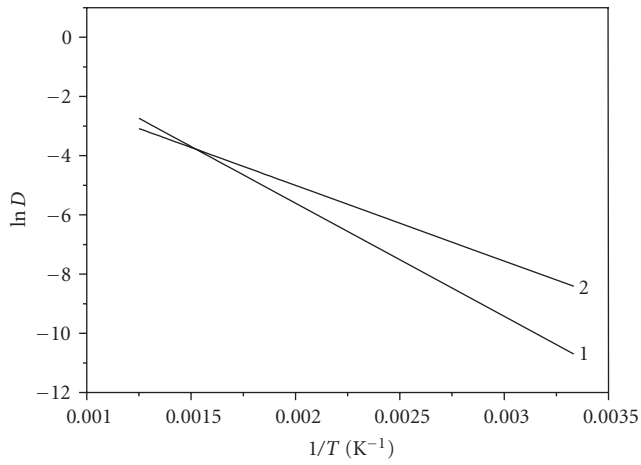

Figure 6: Temperature dependences of ln D versus $1/T$ for sample A (curve 1) and sample B (curve 2).

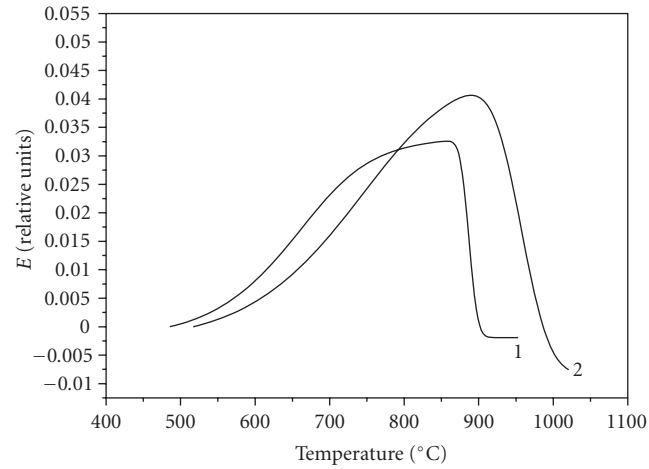

Figure 7: Model curves of the temperature dependences of the radon release rate $E(T)$ for sample A (curve 1) and sample B (curve 2).

diffusion. The temperature dependences of radon release rate, E_D due to diffusion, were calculated using (2). The temperature dependences of $\Psi(T)$ functions, that characterized the annealing of surface and subsurface structure irregularities, were calculated using (3).

Figure 6 depicts temperature dependences of ln D versus $1/T$ calculated from the DSA results measured on heating of sample A and sample B in the temperature range 50–450°C. The determined values of the radon permeability characteristics (activation energy Q_D of the radon diffusion) and the

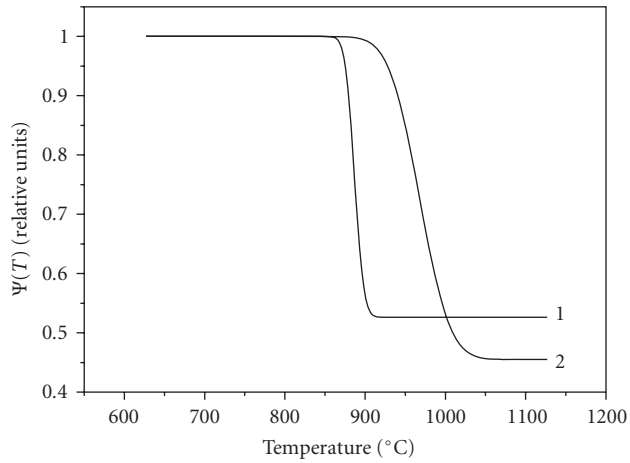

FIGURE 8: Temperature dependences of the functions $\Psi(T)$ for sample A (curve 1) and sample B (curve 2).

pre-exponential factor D_0 are presented in Table 2. Figure 7 depicts the model curves of the temperature dependences of the radon release rate $E(T)$ calculated from the DSA experimental results in the range 500–1050°C. The functions $\Psi(T)$ were used to characterize the annealing of subsurface structure irregularities in the titania powders (samples A and B) during heating in air. Figure 8 depicts the calculated temperature dependences of the functions $\Psi(T)$ for samples A and B. As it follows from Figure 8, the maximum rate of the radon release rate decrease due to annealing of subsurface structure irregularities was determined at 886°C for sample A and 997°C for sample B. Radon atoms have been used in this study as a probe of the nanostructure changes.

4. CONCLUSIONS

Thermal behavior of N-doped titania powders prepared by heat treatment of anatase in gaseous ammonia at 575°C was characterized by diffusion structural analysis (DSA). The radon permeability in the N-doped titania as well as in the reference nondoped titania powder was evaluated from the DSA results. The decrease of the radon release rate observed in the temperature range 850–1000°C made it possible to characterize annealing of microstructure irregularities.

ACKNOWLEDGMENTS

This work was supported in part by the Ministry of Education of the Czech Republic (Projects LA 292 and 1M4531433201) and Ministry for Science, Education, Sports and Culture of Japan.

REFERENCES

[1] A. Fujishima and K. Honda, "Electrochemical photolysis of water at a semiconductor electrode," *Nature*, vol. 238, pp. 37–38, 1972.

[2] A. Sobczyński and A. Dobosz, "Water purification by photocatalysis on semiconductors," *Polish Journal of Environmental Studies*, vol. 10, no. 4, pp. 195–205, 2001.

[3] J. Peral, X. Domènech, and D. F. Ollis, "Heterogeneous photocatalysis for purification, decontamination and deodorization of air," *Journal of Chemical Technology and Biotechnology*, vol. 70, no. 2, pp. 117–140, 1997.

[4] N. Getoff, "Purification of drinking-water by irradiation—a review," in *Proceedings of the Indian Academy of Sciences-Chemical Sciences*, vol. 105, pp. 373–391, Bangalore, India, January-December 1993.

[5] T. Kudo, Y. Kudo, A. Ruike, A. Hasegawa, M. Kitano, and M. Anpo, "The design of highly active rectangular column-structured titanium oxide photocatalysts and their application in purification systems," *Catalysis Today*, vol. 122, no. 1-2, pp. 14–19, 2007.

[6] Y. Cong, L. Xiao, J. Zhang, F. Chen, and M. Anpo, "Preparation and characterization of nitrogen-doped TiO_2 photocatalyst in different acid environments," *Research on Chemical Intermediates*, vol. 32, no. 8, pp. 717–724, 2006.

[7] M. Kitano, K. Tsujimaru, and M. Anpo, "Decomposition of water in the separate evolution of hydrogen and oxygen using visible light-responsive TiO_2 thin film photocatalysts: effect of the work function of the substrates on the yield of the reaction," *Applied Catalysis A*, vol. 314, no. 2, pp. 179–183, 2006.

[8] J. Zhu, F. Chen, J. Zhang, H. Chen, and M. Anpo, "Fe^{3+}-TiO_2 photocatalysts prepared by combining sol-gel method with hydrothermal treatment and their characterization," *Journal of Photochemistry and Photobiology A*, vol. 180, no. 1-2, pp. 196–204, 2006.

[9] M. Anpo and M. Takeuchi, "The design and development of highly reactive titanium oxide photocatalysts operating under visible light irradiation," *Journal of Catalysis*, vol. 216, no. 1-2, pp. 505–516, 2003.

[10] T. Ihara, M. Miyoshi, M. Ando, S. Sugihara, and Y. Iriyama, "Preparation of a visible-light-active TiO_2 photocatalyst by RF plasma treatment," *Journal of Materials Science*, vol. 36, no. 17, pp. 4201–4207, 2001.

[11] Y. Sakatani, H. Ando, K. Okusako, et al., "Metal ion and N co-doped TiO_2 as a visible-light photocatalyst," *Journal of Materials Research*, vol. 19, no. 7, pp. 2100–2108, 2004.

[12] Y. Sakatani, J. Nunoshige, H. Ando, et al., "Photocatalytic decomposition of acetaldehyde under visible light irradiation over La^{3+} and N Co-doped TiO_2," *Chemistry Letters*, vol. 32, no. 12, pp. 1156–1157, 2003.

[13] K. Takeuchi, I. Nakamura, O. Matsumoto, S. Sugihara, M. Ando, and T. Ihara, "Preparation of visible-light-responsive titanium oxide photocatalysts by plasma treatment," *Chemistry Letters*, no. 12, pp. 1354–1355, 2000.

[14] R. Asahi, T. Morikawa, T. Ohwaki, K. Aoki, and Y. Taga, "Visible-light photocatalysis in nitrogen-doped titanium oxides," *Science*, vol. 293, no. 5528, pp. 269–271, 2001.

[15] M. Mrowetz, W. Balcerski, A. J. Colussi, and M. R. Hoffmann, "Oxidative power of nitrogen-doped TiO_2 photocatalysts under visible illumination," *Journal of Physical Chemistry B*, vol. 108, no. 45, pp. 17269–17273, 2004.

[16] T. Ohno, M. Akiyoshi, T. Umebayashi, K. Asai, T. Mitsui, and M. Matsumura, "Preparation of S-doped TiO_2 photocatalysts and their photocatalytic activities under visible light," *Applied Catalysis A*, vol. 265, no. 1, pp. 115–121, 2004.

[17] T. Ohno, T. Mitsui, and M. Matsumura, "Photocatalytic activity of S-doped TiO_2 photocatalyst under visible light," *Chemistry Letters*, vol. 32, no. 4, pp. 364–365, 2003.

[18] S. Sakthivel and H. Kisch, "Daylight photocatalysis by carbon-modified titanium dioxide," *Angewandte Chemie International Edition*, vol. 42, no. 40, pp. 4908–4911, 2003.

[19] T. Umebayashi, T. Yamaki, H. Itoh, and K. Asai, "Band gap narrowing of titanium dioxide by sulfur doping," *Applied Physics Letters*, vol. 81, no. 3, p. 454, 2002.

[20] T. Umebayashi, T. Yamaki, S. Tanaka, and K. Asai, "Visible light-induced degradation of methylene blue on S-doped TiO_2," *Chemistry Letters*, vol. 32, no. 4, pp. 330–331, 2003.

[21] H. Irie, S. Washizuka, Y. Watanabe, T. Kako, and K. Hashimoto, "Photoinduced hydrophilic and electrochemical properties of nitrogen-doped TiO_2 films," *Journal of the Electrochemical Society*, vol. 152, no. 11, pp. E351–E356, 2005.

[22] H. Irie, Y. Watanabe, and K. Hashimoto, "Carbon-doped anatase TiO_2 powders as a visible-light sensitive photocatalyst," *Chemistry Letters*, vol. 32, no. 8, pp. 772–773, 2003.

[23] H. Irie, Y. Watanabe, and K. Hashimoto, "Nitrogen-concentration dependence on photocatalytic activity of $TiO_{2-x}N_x$ powders," *Journal of Physical Chemistry B*, vol. 107, no. 23, pp. 5483–5486, 2003.

[24] H. Hirashima, H. Imai, M. Y. Miah, I. M. Bountseva, I. N. Beckman, and V. Balek, "Preparation of mesoporous titania gel films and their characterization," *Journal of Non-Crystalline Solids*, vol. 350, pp. 266–270, 2004.

[25] V. Balek, T. Mitsuhashi, I. M. Bountseva, H. Haneda, Z. Malek, and J. Šubrt, "Diffusion structural analysis study of titania films deposited by sol-gel technique on silica glass," *Journal of Sol-Gel Science and Technology*, vol. 26, no. 1–3, pp. 185–189, 2003.

[26] V. Balek, J. Šubrt, T. Mitsuhashi, I. N. Beckman, and K. Györyová, "Emanation thermal analysis. Ready to fulfill the future needs of materials characterization," *Journal of Thermal Analysis and Calorimetry*, vol. 67, no. 1, pp. 15–35, 2002.

[27] J. F. Ziegler and J. P. Biersack, *The stopping and range of ions in solids*, Pergamon, New York, NY, USA, 1985.

[28] S. Bakardjieva, J. Šubrt, V. Štengl, M. J. Dianez, and M. J. Sayagues, "Photoactivity of anatase-rutile TiO_2 nanocrystalline mixtures obtained by heat treatment of homogeneously precipitated anatase," *Applied Catalysis B*, vol. 58, no. 3-4, pp. 193–202, 2005.

[29] J. Krýsa, M. Keppert, J. Jirkovský, V. Štengl, and J. Šubrt, "The effect of thermal treatment on the properties of TiO_2 photocatalyst," *Materials Chemistry and Physics*, vol. 86, no. 2-3, pp. 333–339, 2004.

[30] A. Daßler, A. Feltz, J. Jung, W. Ludwig, and E. Kaisersberger, "Characterization of rutile and anatase powders by thermal analysis," *Journal of Thermal Analysis*, vol. 33, no. 3, pp. 803–809, 1988.

[31] V. Balek and I. N. Beckman, "Theory of emanation thermal analysis XII. Modelling of radon diffusion release from disordered solids on heating," *Journal of Thermal Analysis and Calorimetry*, vol. 82, no. 3, pp. 755–759, 2005.

[32] I. N. Beckman and V. Balek, "Theory of emanation thermal analysis. XI. Radon diffusion as the probe of microstructure changes in solids," *Journal of Thermal Analysis and Calorimetry*, vol. 67, no. 1, pp. 49–61, 2002.